Article

SOURCE DATA | TRANSPARENT PROCESS

EMBO reports

# Irgm2 and Gate-16 cooperatively dampen Gram-negative bacteria-induced caspase-11 response

Elif Eren[1,†], Rémi Planès[1,†], Salimata Bagayoko[1], Pierre-Jean Bordignon[1], Karima Chaoui[1,2], Audrey Hessel[1], Karin Santoni[1], Miriam Pinilla[1], Brice Lagrange[3], Odile Burlet-Schiltz[1,2], Jonathan C Howard[4], Thomas Henry[3], Masahiro Yamamoto[5,6] & Etienne Meunier[1,‡,*]

## Abstract

**Inflammatory caspase-11 (rodent) and caspases-4/5 (humans) detect the Gram-negative bacterial component LPS within the host cell cytosol, promoting activation of the non-canonical inflammasome. Although non-canonical inflammasome-induced pyroptosis and IL-1-related cytokine release are crucial to mount an efficient immune response against various bacteria, their unrestrained activation drives sepsis. This suggests that cellular components tightly control the threshold level of the non-canonical inflammasome in order to ensure efficient but non-deleterious inflammatory responses. Here, we show that the IFN-inducible protein Irgm2 and the ATG8 family member Gate-16 cooperatively counteract Gram-negative bacteria-induced non-canonical inflammasome activation, both in cultured macrophages and *in vivo*. Specifically, the Irgm2/Gate-16 axis dampens caspase-11 targeting to intracellular bacteria, which lowers caspase-11-mediated pyroptosis and cytokine release. Deficiency in *Irgm2* or *Gate16* induces both guanylate binding protein (GBP)-dependent and GBP-independent routes for caspase-11 targeting to intracellular bacteria. Our findings identify molecular effectors that fine-tune bacteria-activated non-canonical inflammasome responses and shed light on the understanding of the immune pathways they control.**

**Keywords** Caspase-11; Gate-16; infections/Interferons; Irgm2; non-canonical inflammasome

**Subject Categories** Autophagy & Cell Death; Immunology; Microbiology, Virology & Host Pathogen Interaction

**DOI** 10.15252/embr.202050829 | Received 7 May 2020 | Revised 11 September 2020 | Accepted 25 September 2020 | Published online 30 October 2020

**EMBO Reports (2020) 21: e50829**

See also: **R Finethy *et al*** and **A Linder & V Hornung** (November 2020)

## Introduction

Inflammasomes are cytosolic innate immune complexes that initiate inflammatory responses upon sensing of microbe- and damage-associated molecular patterns (MAMPs and DAMPs, respectively) (Hayward *et al*, 2018). Specifically, the rodent caspase-11 (and its human orthologs caspase-4 and caspase-5) detects the presence of the Gram-negative bacterial cell wall component lipopolysaccharide (LPS) within the host cell cytosol (Kayagaki *et al*, 2011, 2013; Broz *et al*, 2012; Aachoui *et al*, 2013; Hagar *et al*, 2013; Yang *et al*, 2015). LPS interaction with the caspase activation and recruitment domain (CARD) of caspase-11 promotes its oligomerization and activation, which triggers the activation of the non-canonical inflammasome (Yang *et al*, 2015). Upon activation (Lee *et al*, 2018), caspase-11 cleaves and activates the pyroptosis executioner gasdermin-D (gsdmD) into the p30 active fragment (Kayagaki *et al*, 2015; Shi *et al*, 2015). Cleaved gsdmD then forms a pore into phosphatidylinositol-4,5-bisphosphate (PIP2)-enriched domains at the plasma membrane, which triggers pyroptosis, a pro-inflammatory form of cell death (Shi *et al*, 2015; Aglietti *et al*, 2016; Liu *et al*, 2016; Sborgi *et al*, 2016). In parallel, gsdmD pore-induced ionic perturbations also trigger activation of the canonical NLRP3 inflammasome, which results in the caspase-1-dependent maturation of the pro-inflammatory cytokines interleukins (IL)-1β and IL-18 (Kayagaki *et al*, 2011; Rühl & Broz,

1 Institute of Pharmacology and Structural Biology (IPBS), CNRS, UMR5089, University of Toulouse, Toulouse, France
2 Mass Spectrometry Core Facility, Institute of Pharmacology and Structural Biology (IPBS), CNRS, UMR5089, University of Toulouse, Toulouse, France
3 CIRI, Centre International de Recherche en Infectiologie, Inserm, U1111, CNRS, UMR5308, École Normale Supérieure de Lyon, Université Claude Bernard Lyon 1, Univ Lyon, Lyon, France
4 Fundação Calouste Gulbenkian, Instituto Gulbenkian de Ciência, Oeiras, Portugal
5 Department of Immunoparasitology, Research Institute for Microbial Diseases, Osaka University, Osaka, Japan
6 Laboratory of Immunoparasitology, WPI Immunology Frontier Research Center, Osaka University, Osaka, Japan
*Corresponding author. Tel: +33 0 561175832; E-mail: etienne.meunier@ipbs.fr
†These authors contributed equally to this work
‡Present Address: Institute of Pharmacology and Structural Biology (IPBS), CNRS, Toulouse, France

2015; Schmid-Burgk *et al*, 2015). Although caspase-11 confers host protection against intracellular Gram-negative bacteria (Aachoui *et al*, 2013; Cerqueira *et al*, 2018; Chen *et al*, 2018), its unrestrained activation provokes irreversible organ failure, blood clothing and sepsis (Kayagaki *et al*, 2011, 2013, 2015; Napier *et al*, 2016; Cheng *et al*, 2017; Deng *et al*, 2018; Rathinam *et al*, 2019; Yang *et al*, 2019). This suggests that host regulators might fine-tune the non-canonical inflammasome in order to optimize caspase-11-dependent response. To date, only few of them were described including SERPINB1-inhibited caspase-11/-4/-1 activation in resting cells or ESCRT-mediated plasma membrane repair (Rühl *et al*, 2018; Choi *et al*, 2019).

Crucial at regulating the activation the non-canonical inflammasome pathway are the IFN-inducible GTPases, the so-called guanylate binding proteins (GBPs) and the immunity-related GTPase (Irg) Irgb10 (Meunier *et al*, 2014, 2015; Pilla *et al*, 2014; Finethy *et al*, 2015; Man *et al*, 2015, 2016; Wallet *et al*, 2017; Zwack *et al*, 2017; Cerqueira *et al*, 2018; Costa Franco *et al*, 2018; Lagrange *et al*, 2018; Liu *et al*, 2018). Specifically, GBPs (1, 2, 3, 4 and 5) are recruited on LPS-enriched structures such as cytosolic Gram-negative bacteria and their derived products outer membrane vesicles (OMVs) (Meunier *et al*, 2014; Man *et al*, 2015; Finethy *et al*, 2017; Lagrange *et al*, 2018; Santos *et al*, 2018; Fisch *et al*, 2019). As such, these GBPs then engage caspase-11 that will bind the LPS moiety lipid A, hence promoting the non-canonical inflammasome pathway (Fisch *et al*, 2019). Beyond their role at triggering GBP expression, IFNs induce more than 2,000 antimicrobial genes (Green *et al*, 2018). Among them, many IFN-inducible regulatory genes also counter-balance overactivation of the cells (Green *et al*, 2018). For instance, SOCS1 and USP18 are ISGs that balance the level of the host cell response (Basters *et al*, 2018; Liau *et al*, 2018). In this context, we hypothesized that IFNs, in addition to their ability to promote GBP expression, might also induce negative regulators of the non-canonical inflammasome. In this regard, Irgm proteins belong to the IFN-inducible immunity-related GTPase (Irg) family proteins (Kim *et al*, 2012, 2019; Pilla-Moffett *et al*, 2016). Human being possess one IRGM protein, with various spliced variants, that is not IFN-inducible but that requires IFN signalling to be functional (Kim *et al*, 2019). By contrast, mice display three different Irgms, namely Irgm1, Irgm2 and Irgm3 (Kim *et al*, 2012). All Irgms lack the ability to hydrolyse the GTP due to a mutation in their catalytic domain (GMS), whereas other Irgs are GTPase active (GKS) (Coers, 2013). Previous studies underscored an inhibitory role of Irgm1 and Irgm3 on the recruitment and/or activation of the GBPs and Irg-GKS on microbial membranes although independent processes can also occur (Haldar *et al*, 2013, 2015; Feeley *et al*, 2017). In addition, recent studies identified Irgm1 and its human homologous IRGM, as being critical for the NLRP3 canonical inflammasome regulation by modulating the autophagy pathway, suggesting a close link between Irgm proteins and inflammasomes (Pei *et al*, 2017; Mehto *et al*, 2019a, b). In this context, we hypothesized that Irgm proteins might be IFN-inducible regulators of the non-canonical inflammasome activation threshold.

Here, we report that IFN-inducible Irgm2 and the non-canonical autophagy effector Gate-16 indirectly fine-tune non-canonical inflammasome activation by intracellular bacteria, which protects against endotoxemia.

## Results and Discussion

### IFN-inducible protein Irgm2 restrains Caspase-11-dependent responses to Gram-negative bacteria

IFN-inducible Irgms control Irg and GBP microbicidal activity against intracellular pathogens (Pilla-Moffett *et al*, 2016). In this context, we sought to determine whether Irgms might also modulate the non-canonical inflammasome response. Using an RNA interference approach (siRNA), we silenced the three murine Irgms in primary murine bone marrow-derived macrophages (BMDMs) and measured their ability to undergo caspase-11-dependent cell death and IL-1β maturation upon *Salmonella* Typhimurium challenge. To ensure that the inflammasome response in macrophages is caspase-11-dependent, we used an isogenic mutant of *Salmonella* (*orgA*$^-$) lacking expression of SP1-encoded T3SS secretion system (Broz *et al*, 2012). As previously published, *Casp11* and *Gbp2* silencing reduced macrophage death (LDH release) and IL-1β release after 16 h of infection (Figs 1A and EV1A; Meunier *et al*, 2014). Importantly, *Irgm2*-silenced BMDMs had higher levels of cell death and IL-1β release than the wild-type (WT) macrophages (Figs 1A and EV1A). Such process was specific to Irgm2 given that *Irgm1*- and *Irgm3*-targeted siRNAs did not induce significant variation in macrophage death and IL-1β release upon *Salmonella* (*orgA*$^-$) infection, despite the fact that their mRNA levels were efficiently reduced (Figs 1A and EV1A). To further validate that Irgm2 is a regulator of the non-canonical inflammasome response, we challenged WT, *Irgm2*$^{-/-}$, *Casp11*$^{-/-}$ and *GBP*$^{Chr3-/-}$ BMDMs with a panel of Gram-negative bacteria all known to activate the non-canonical inflammasome. Immunoblotting experiments in WT and *Irgm2*$^{-/-}$ BMDMs showed that Irgm2 is IFN-inducible and that *Irgm2* deficiency does not lead to a defect in caspase-1, caspase-11, GBP2 or GBP5 expression, all involved in the non-canonical inflammasome pathway (Fig EV1B and C). Yet, when challenged with various Gram-negative bacteria, *Irgm2*$^{-/-}$ macrophages showed an exacerbated cell death, IL-1β release and gasdermin-D p30 (active) and processed caspase-1 p20 (inactive) fragments compared with their WT counterparts (Fig 1B and C). In addition, Irgm2-regulated cell pyroptosis upon Gram-negative bacterial challenge was independent of NLRP3 as the use of the NLRP3 inhibitor MCC950 or *Nlrp3*$^{-/-}$ BMDMs did not drive any defect in cell death but significantly reduced NLRP3-dependent IL-1β release (Fig EV1D). As expected, both *Casp11*$^{-/-}$ and *GBP*$^{Chr3-/-}$ BMDMs were protected against Gram-negative bacteria-induced non-canonical inflammasome response (Fig 1B). Importantly, CRISPR-deleted *Irgm2* gene expression in immortalized (i) *Casp11*$^{-/-}$ BMDMs (referred as *Casp11*$^{-/-}$ sg*Irgm2*) did not reinduce pyroptosis and IL-1β release upon Gram-negative bacterial infections (*S.* Typhimurium *orgA*$^-$ and *Escherichia coli*) or *E. coli*-derived OMVs exposure, thus confirming that Irgm2 negatively regulated caspase-11-dependent response (Figs 1D and EV1E). Next, we assessed whether Irgm2 directly or indirectly regulates the non-canonical inflammasome response. To this end, we electroporated LPS into the host cell cytosol of IFNγ-primed WT, *Irgm2*$^{-/-}$ and *Casp11*$^{-/-}$ BMDMs and evaluated their ability to undergo pyroptosis. Surprisingly, we observed that WT and *Irgm2*$^{-/-}$ macrophages engaged cell death to the same extent 4 h after LPS electroporation whereas *Casp11*$^{-/-}$ BMDMs were protected against LPS-induced cell death (Fig 1E). This suggests that

 

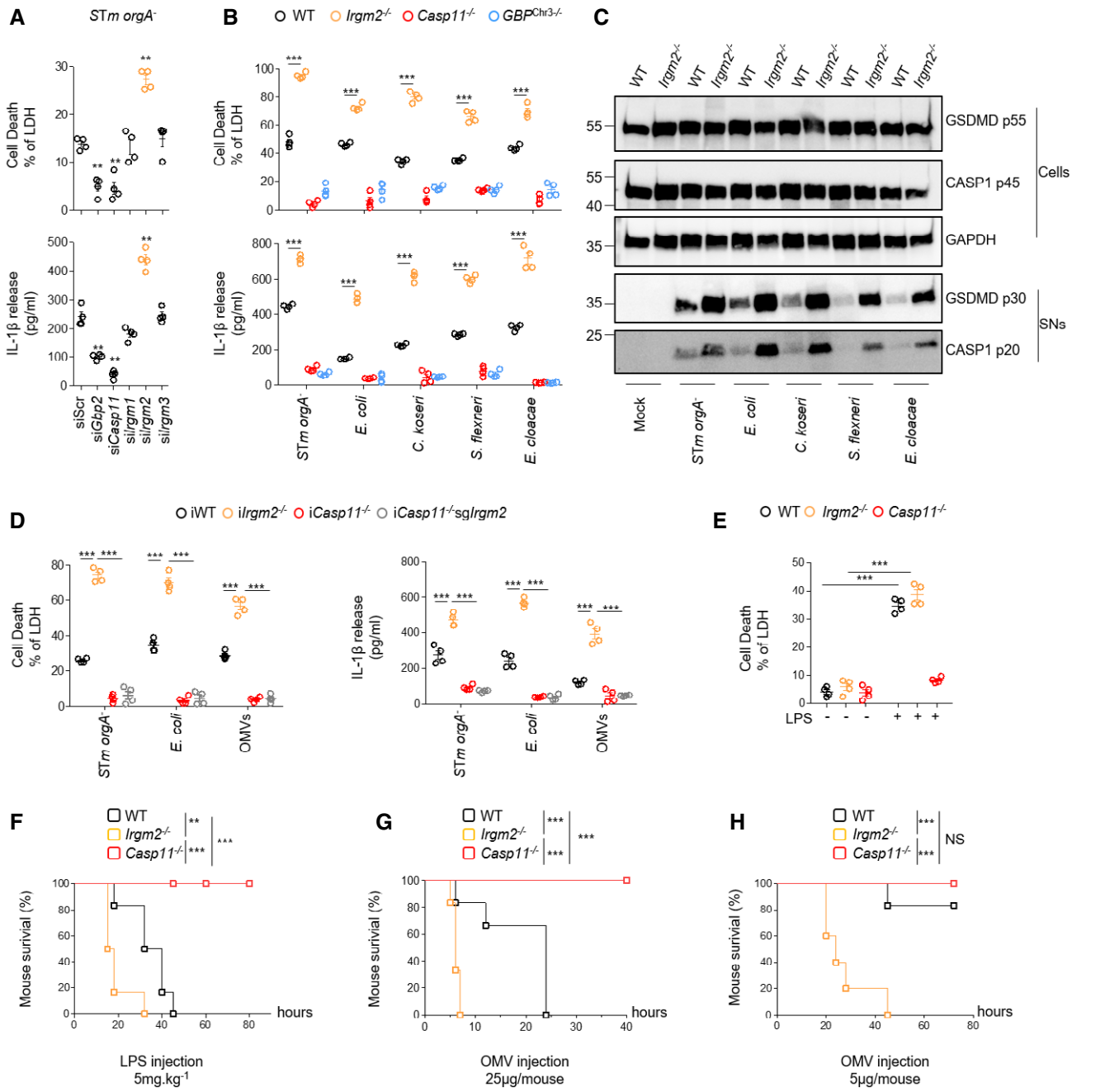


**Figure 1. IFN-inducible protein Irgm2 restrains caspase-11-dependent response to Gram-negative bacteria.**

Unless otherwise specified, BMDMs were either infected with various Gram-negative bacterial strains (MOI25) or stimulated with outer membrane vesicles (OMVs) for 16 h.

A siRNA-treated BMDMs were infected for 16 h with *S.* Typhimurium (*orgA*$^{-}$), and LDH and IL-1β release were measured.

B Cell death (LDH) and IL-1β release evaluation in WT, *Irgm2*$^{-/-}$, *GBP*$^{Chr3-/-}$ and *Casp11*$^{-/-}$ BMDMs infected for 16 h with different Gram-negative bacteria (MOI 25).

C Western blot examination of processed caspase-1 (p20) and gasdermin-D (p30) in supernatants and pro-caspase-1 (p45), pro-gasdermin-D (p55) and GAPDH in cell lysates of WT and *Irgm2*$^{-/-}$ BMDMs infected for 16 h with different Gram-negative bacterial strains.

D IL-1β and cell death (% LDH) evaluation in immortalized WT, *Irgm2*$^{-/-}$, *Casp11*$^{-/-}$ and *Casp11*$^{-/-}$*Irgm2*$^{-/-}$ (referred as sg*Irgm2*) BMDMs after 16 h of *Escherichia coli*, *S.* Typhimurium *orgA*$^{-}$ and OMV treatment.

E Cell death (% LDH) evaluation in IFNγ-primed WT, *Irgm2*$^{-/-}$ and *Casp11*$^{-/-}$ BMDMs 4 h after electroporation or not with 1 µg of *E. coli* LPS.

F–H Survival of WT, *Casp11*$^{-/-}$ and *Irgm2*$^{-/-}$ mice primed with 100 µg poly(I:C) for 6 h and injected (i.p.) with 5 mg/kg LPS or 5 and 25 µg of OMVs ($n$ = 6 animals per condition).

Data information: Data shown as means ± SEM (graphs A, B, D and E) from $n$ = 4 independent pooled experiments; $^{**}P \leq 0.01$, $^{***}P \leq 0.001$ for the indicated comparisons using $t$-test with Bonferroni correction. Image (C) is representative of one experiment performed three times. (F–H) are representative of three independent experiments; $^{*}P \leq 0.05$; $^{**}P \leq 0.01$, $^{***}P \leq 0.001$, log-rank Cox–Mantel test for survival comparisons (F–H).
Source data are available online for this figure.

Irgm2-inhibited caspase-11 response occurs upstream from LPS sensing by caspase-11.

Based on these results, we next determined whether Irgm2 also inhibited canonical inflammasomes. We treated WT, *Irgm2*$^{-/-}$, *Casp11*$^{-/-}$ and *Casp1*$^{-/-}$*Casp11*$^{-/-}$ BMDMs with various inflammasome activators, including flagellin (NLRC4), poly-dAdT (AIM2), Nigericin (NLRP3) and TcdB (PYRIN), and measured their ability to commit pyroptosis and to release IL-1β. Although all canonical inflammasome activators induced significant caspase-1-dependent response, cell death and IL-1β release levels remained similar in both WT and *Irgm2*$^{-/-}$ BMDMs (Fig EV1F). In addition, activation of the NLRC4 inflammasome by T3SS-expressing *Pseudomonas aeruginosa* and *S*. Typhimurium remained similar between WT and *Irgm2*$^{-/-}$ BMDMs (Fig EV1G), suggesting that Irgm2 specifically regulates the non-canonical inflammasome response to Gram-negative bacteria.

As caspase-11 also drives mouse susceptibility to LPS-induced inflammatory-related damages, we also evaluated whether *Irgm2* deficiency might sensitize mice to sepsis. We used two LPS-dependent sepsis models, where WT, *Irgm2*$^{-/-}$ and *Casp11*$^{-/-}$ mice were intraperitoneally injected with poly(IC) to induce ISG expression (Kayagaki *et al*, 2013; Santos *et al*, 2018). Then, mice were injected either with pure LPS (5 mg/kg) or with OMVs (25 μg/ml; Vanaja *et al*, 2016; Santos *et al*, 2018). Mouse survival showed that while *Casp11*$^{-/-}$ mice had resistance to LPS- and OMV-induced sepsis, WT mice succumbed faster, hence validating our sepsis model (Fig 1F and G). Noticeably, *Irgm2*$^{-/-}$ mice were even more susceptible than WT mice to both LPS- and OMV-induced sepsis (Fig 1F and G). Therefore, we used a sub-lethal model of OMV-induced sepsis by injecting 5 μg of OMVs in mice. In such model, both WT and *Casp11*$^{-/-}$ mice recovered from OMV injection whereas all *Irgm2*$^{-/-}$ mice did succumb (Fig 1H). Moreover, cytokine assays showed that *Irgm2*$^{-/-}$ mice had an exacerbated release of all pro-inflammatory and inflammasome-related cytokines tested upon OMV challenge, a phenotype that was reduced in *Casp11*$^{-/-}$ mice, hence confirming that Irgm2 expression is crucial to temperate the activation level of the non-canonical inflammasome (Fig EV1H). Altogether, our data suggest that Irgm2 indirectly inhibits caspase-11-dependent endotoxemia, which protects against sepsis.

### Irgm2 regulates GBP-independent caspase-11 targeting to Gram-negative bacteria

IFN-inducible GBPs are important regulators of the non-canonical inflammasome response. Specifically, GBP-1 and GBP-2 regulate human caspase-4/-5 activation while GBP-2 and GBP-5 control mouse caspase 11. Therefore, we hypothesized that Irgm2 might control caspase-11 response through the modulation of the GBPs. To this end, we silenced *Irgm2* in WT and *GBP*$^{Chr3-/-}$ BMDMs (lacking 5 GBPs, 1-3, 5 and 7) and evaluated the caspase-11 response upon OMV stimulation (Fig EV2A). While OMV-induced both cell death and IL-1β release was strongly reduced in *GBP*$^{Chr3-/-}$, *Irgm2*-silenced *GBP*$^{Chr3-/-}$ BMDMs partially recovered a caspase-11-dependent response, suggesting that Irgm2-inhibited caspase-11 response could occur independently of GBPs (Fig 2A). Other and we previously showed that GBPs also controlled canonical AIM2 inflammasome activation upon *Francisella tularensis* spp *novicida* infection. In this context, we evaluated the importance of Irgm2 at controlling AIM2 inflammasome response upon *F. novicida* infection. Surprisingly, IL-1β and cell death levels were not different between WT and *Irgm2*$^{-/-}$, although they were strongly reduced in *Casp1*$^{-/-}$*Casp11*$^{-/-}$ and *GBP*$^{Chr3-/-}$ BMDMs (Figs 2B and EV2B). In addition, we observed that *Irgm2*-silenced *GBP*$^{Chr3-/-}$ BMDMs did not recover an inflammasome response upon *F. novicida* infection. Then, we generated i*GBP*$^{Chr3-/-}$ *Irgm2*$^{-/-}$ (referred hereafter as i*GBP*$^{Chr3-/-}$sg*Irgm2*) by crispr Cas9 and evaluated their response upon *S*. Tm (*orgA*$^{-}$) challenge. i*Irgm2*$^{-/-}$ BMDMs showed time-dependent increased cell death compared with iWT cells (Fig EV2C and D). While cell death in i*GBP*$^{Chr3-/-}$ BMDMs was strongly impaired, it was partially reversed in i*GBP*$^{Chr3-/-}$sg*Irgm2*, alluding that *Irgm2* deficiency was sufficient to specifically promote caspase-11-dependent response in the absence of GBPs (Fig EV2C and D). GBP enrichment on microbial ligand is of importance for efficient caspase-11 and human caspase-4 recruitment (Thurston *et al*, 2016; Fisch *et al*, 2019). However, monitoring for GBP loading on mCherry-expressing *S*. Typhimurim did not show a significant change in the percentage of bacteria targeted by GBP2 (10–15%) in WT and *Irgm2*$^{-/-}$ BMDMs (Fig 2C), which suggests that Irgm2-inhibited non-canonical inflammasome response does not involve GBP2 recruitment modulation.

As caspase-11 activation needs binding to LPS, we hypothesized that Irgm2 expression regulates caspase-11 recruitment to bacterial LPS. In order to monitor this, we generated WT, *Irgm2*$^{-/-}$, *GBP*$^{Chr3-/-}$ and *GBP*$^{Chr3-/-}$*Irgm2*$^{-/-}$ iBMDMs that expressed a catalytically inactive mutant of caspase-11 coupled to GFP (Thurston *et al*, 2016) and primed them with IFNγ to induce ISG expression. The recruitment of CASP11-C254G-GFP on *S*. Typhimurium (*orgA*$^{-}$) occurred after 4 h of infection in *Irgm2*$^{-/-}$ iBMDMs, whereas the percentage of caspase-11-targeted bacteria in iWT *GBP*$^{Chr3-/-}$ and *GBP*$^{Chr3-/-}$*Irgm2*$^{-/-}$ iBMDMs remained low or null (Fig EV2E). After 8 h of infection, however, the levels of CASP11-C254G-GFP-associated bacteria increased in iWT (10%), albeit the percentage of CASP11-C254G-GFP$^{+}$ bacteria remained below those observed in *Irgm2*$^{-/-}$ cells (15–16%) (Fig 2D). Strikingly, we noticed that CASP11-C254G-GFP targeting to *Salmonella* was partially restored in *GBP*$^{Chr3-/-}$*Irgm2*$^{-/-}$ iBMDM after 8 h of infection, although it was strongly impaired in *GBP*$^{Chr3-/-}$ cells (Fig 2D). Altogether, our results point out that *Irgm2* deficiency accelerates caspase-11 recruitment on bacterial membranes. Although we cannot entirely exclude that Irgm2 might also regulate GBP-dependent caspase-11 recruitment to bacterial membranes, our result show that an *Irgm2* deficiency opens a GBP$^{Chr3}$ alternative road for caspase-11 response.

### Irgm2 cooperates with GATE16 to dampen Gram-negative bacteria-induced non-canonical inflammasome activation

As *Irgm2* deficiency can promote caspase-11 activation independently of *GBP*$^{Chr3}$, we next searched for additional regulators. We used a GFP-Trap coupled to mass spectrometry (MS) strategy using IFNγ-primed i*Irgm2*$^{-/-}$ BMDMs complemented with a doxycycline-inducible Irgm2-GFP construct (Fig 3A). Although we detected some important described immune regulators (e.g., galectin-8), the three independent MS datasets (Fig EV3A) showed that one protein, namely gamma-aminobutyric acid (GABA)-A-receptor-associated protein (GabarapL2, referred as Gate-16), was reproducibly enriched in the top 10 hits of the Irgm2-GFP fraction (Figs 3A and EV3A). Therefore, we decided to investigate whether Gate-16 played a role in Irgm2-inhibited caspase-11 response. Co-immunoprecipitation

 

experiments confirmed that Gate-16 was present in the Irgm2-GFP fraction, hence validating our MS results (Fig 3B). Gabarap proteins (Gabarap, GabarapL1 and Gate-16) belong to the ATG8 superfamily proteins, all involved in autophagy/membrane remodelling regulation. While *Gabarap* deficiency leads to increased canonical NLRP3 inflammasome response in mice, there is no information regarding the putative function of Gate-16 at regulating the non-canonical inflammasome. In this context, we found that silencing of *Gate-16*, but no other *gabaraps,* increased OMV-induced caspase-11-dependent cell death and IL-1β release (Figs 3C, and EV3B and C). As a control, *Gate-16* silencing did not alter BMDM response to canonical NLRP3 inflammasome activators (Fig EV3D). Then, we sought to determine whether Gate-16-inhibited caspase-11 response was part of the Irgm2 path. Consequently, we silenced *Gate-16* gene expression in WT, $GBP^{Chr3-/-}$, $Casp11^{-/-}$ and $Irgm2^{-/-}$ BMDMs and evaluated the ability of OMVs to induce a caspase-11-dependent response. *Gate-16*

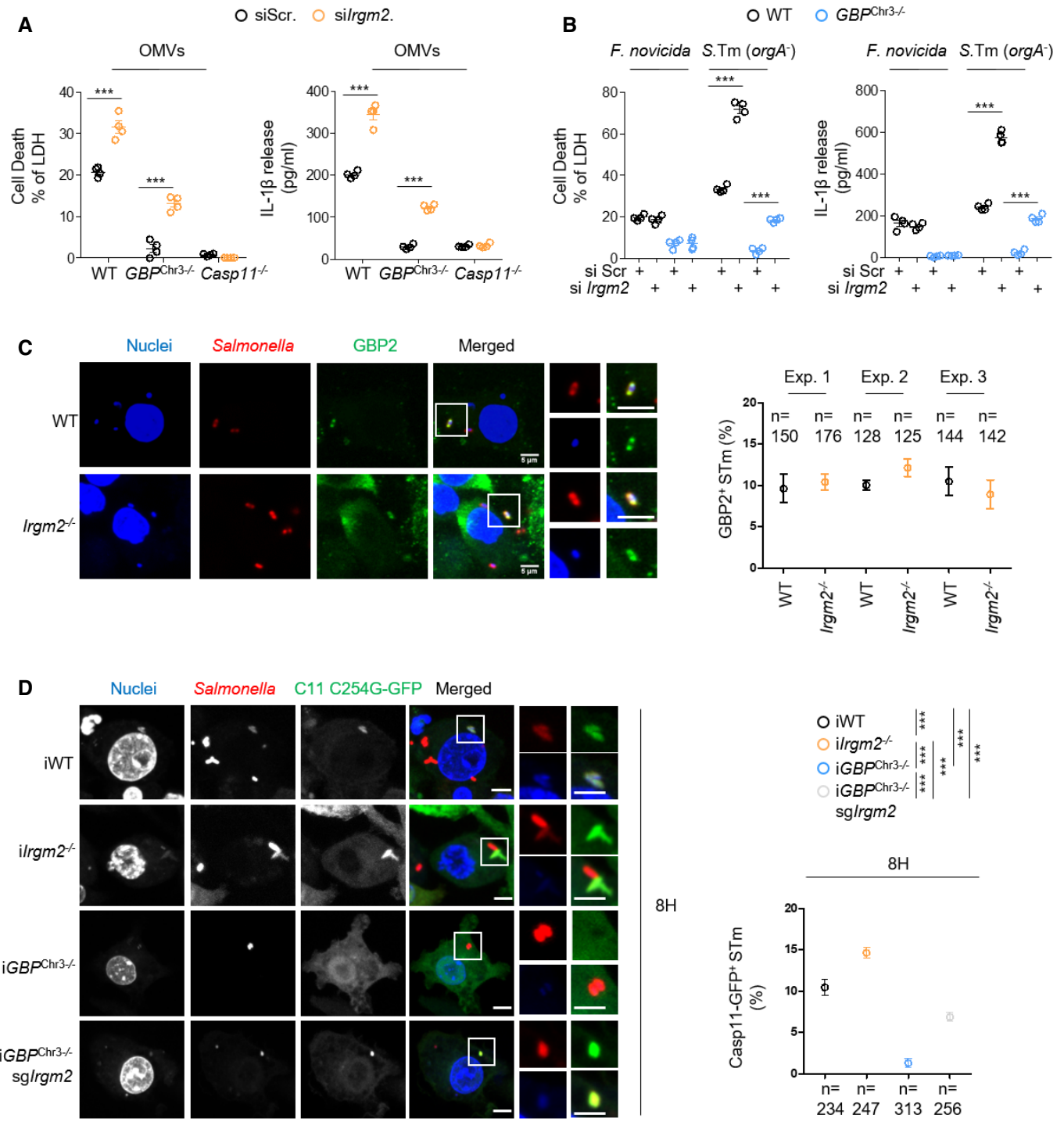


**Figure 2.**

**Figure 2. Irgm2 regulates GBP-independent caspase-11 targeting to Gram-negative bacteria.**

Unless otherwise specified, BMDMs were treated with 2.5 μg/2 × $10^5$ cells of OMVs or infected with either *S.* Typhimurium *orgA*$^-$ (*S.* Tm *orgA*$^-$) or *F. tularensis* spp *novicida* (*F. novicida*) with an MOI of 25 for various times.

A Measure of LDH and IL-1β release in WT, *GBP*$^{Chr3-/-}$ and *Casp11*$^{-/-}$ BMDMs were Irgm2 was knocked down 16 h after exposure to 2.5 μg/2 × $10^5$ cells of OMVs. Si Scramble (siScr.) refers to RNAi pools with non-targeting sequences.

B Cell death (LDH) and IL-1β release evaluation in *Irgm2*-silenced WT and *GBP*$^{Chr3-/-}$ BMDMs infected for 16 h with either *S.* Tm *orgA*$^-$ or *F. novicida* (MOI 25). Si Scramble (siScr.) refers to RNAi pools with non-targeting sequences.

C Florescence microscopy and associated quantifications of GBP-2 (green) recruitments to intracellular *S.* Tm *orgA*$^-$-mCherry (MOI 10, red) in IFNγ-primed WT and *Irgm2*$^{-/-}$ BMDMs. Nucleus was stained with Hoechst (blue). Confocal images shown are from one experiment and are representative of $n = 3$ independent experiments; scale bars 5 μm. For quantifications, the percentage of GBP-associated bacteria was quantified and "*n*=" refers to the number of intracellular bacteria counted in each experiment; quantifications from $n = 3$ independent experiments were then plotted and expressed as mean ± SEM.

D Confocal fluorescence microscopy images and associated quantifications of caspase-11-C254G-GFP (green) recruitment to *S.* Tm-mCherry (*orgA*$^-$, red) in IFNγ-primed iWT, i*Irgm2*$^{-/-}$, i*GBP*$^{Chr3-/-}$ and i*GBP*$^{Chr3-/-}$/sg*Irgm2* BMDMs after 8 h of infection. Nucleus (blue) was stained with Hoescht, scale bar 5 μm. For quantifications, the percentage of bacteria positive for caspase-11-C254G-GFP was determined by combining the bacterial counts from $n = 3$ independent experiments and expressed as mean ± SEM. ***$P \leq 0.001$ for the indicated comparisons using *t*-test with Bonferroni correction.

Data information: Data shown as means ± SEM (graphs A, B) from $n = 4$ independent pooled experiments; ***$P \leq 0.001$ for the indicated comparisons using *t*-test with Bonferroni correction. Images (C, D) are representative of one experiment performed three times.

silencing in WT BMDMs increased the non-canonical inflammasome response while *Casp11*$^{-/-}$ macrophages remained unresponsive to OMV-induced cell death, IL-1β release (Fig 3D). Interestingly, we observed that *GBP*$^{Chr3-/-}$ macrophages silenced for Gate-16 partially recovered their ability to respond to caspase-11 activators (Fig 3E). Finally, *Gate-16* knock down in *Irgm2*$^{-/-}$ BMDMs did not exacerbate cell death and IL-1β release nor gasdermin-D or caspase-1 cleavages (Fig 3D and E), suggesting that Irgm2 and Gate-16 work together to restrain non-canonical inflammasome response. Since *Irgm2* deficiency leads to caspase-11 enrichment to bacterial membranes, we wondered about the role of Gate-16 in this process. We silenced *Gate-16* in iWT-expressing CASP11-C254G-GFP and checked for its recruitment on *S.* Tm membranes. Consequently, iWT BMDMs knocked down for *Gate-16* had a more pronounced accumulation of caspase-11 on *S.* Tm membranes than the controls after 4 and 8 h of infection (Fig 3F), which mirrored what we previously observed in *Irgm2*$^{-/-}$ macrophages. By contrast, *Gate-16* silencing in *Irgm2*$^{-/-}$ did not increase the percentage of bacteria targeted by CASP11-C254G-GFP after 4 h of infection (Fig EV3E). Recent work suggested that caspase-11 activation could restrict *Salmonella* proliferation in macrophages and epithelial cells (Meunier *et al*, 2014; Thurston *et al*, 2016). Therefore, we monitored bacterial load in WT and *Casp11*$^{-/-}$ BMDMs in which we silenced *Irgm2* and *Gate-16*. Whereas *Gate-16* silencing led to slight increased colony forming unit (CFUs) 24 h after infection, *Irgm2* silencing did not modify intracellular bacterial loads, suggesting that Gate-16 also covers a caspase-11-independent cell autonomous immune process (Fig EV3F). Altogether, these results suggest that Irgm2 and Gate-16 cooperate to restrict the non-canonical inflammasome response by restraining caspase-11 targeting to bacterial membranes.

### Irgm2- and Gate16-inhibited *Salmonella*-induced non-canonical inflammasome responses do not involve canonical autophagy

As Gate-16 is involved in the canonical and non-canonical autophagy regulation, we wondered if the exacerbated non-canonical inflammasome response observed in the absence of Gate-16 and Irgm2 relied on autophagy modulation. Therefore, we pharmacologically inhibited canonical autophagy (3-MA or Wortmannin) in WT and *Casp11*$^{-/-}$ BMDMs targeted with siRNA against *Irgm2* or *Gate-16*. Autophagy inhibition in BMDMs triggered exacerbated *Salmonella* (*orgA*$^-$)-induced cell death and IL-1β release, a process that required caspase-11 (Fig EV4A). However, although Irgm2 and Gate16 knock down drove increased caspase-11-dependent response, autophagy inhibition also exacerbated the macrophage response to *Salmonella* infection (Fig EV4A). LC3b targeting to bacteria is also a hallmark of anti-bacterial autophagy (Masud *et al*, 2019; Wu & Li, 2019). Consequently, we infected WT BMDMs silenced for *Irgm2* or *Gate16* with *Salmonella* and analysed by fluorescence microscopy the recruitment of LC3b on bacterial compartments. We found that the percentage of LC3b$^+$ bacteria in control siRNA-treated BMDMs was not significantly altered in BMDMs silenced for *Irgm2* or *Gate16*, although we noticed a trend for LC3b accumulation in si*Gate16*-treated cells (Fig EV4B). This suggests that *Gate16* and *Irgm2* deficiencies modulate the non-canonical inflammasome response independently of canonical autophagy. This is in agreement with the findings of Finethy *et al* (2020) that underlined a lack of canonical autophagy markers (e.g., LC3 lipidation) alteration in *Irgm2*$^{-/-}$ BMDMs. Yet, BMDMs deficient for canonical autophagy regulators had an exacerbated non-canonical inflammasome response. Altogether, these results suggest that Gate-16/Irgm2-inhibited non-canonical inflammasome response does not involve canonical autophagy modulation.

### GATE16 inhibits non-canonical inflammasome activation in human myeloid cells

Gate-16 is expressed in both humans and rodents, yet humans only express one IRGM, although mice have three (Irgm1-3). Therefore, we performed siRNA-based experiments in primary human monocyte-derived macrophages (hMDMs) to determine whether IRGM and GATE16 might also regulate the caspase-4/5 non-canonical inflammasome. Although the use of the caspase-4/5 inhibitor LEVD and of the NLRP3 inhibitor MCC950 showed that hMDMs responded to *Salmonella orgA*$^-$ infection by activating the non-canonical inflammasome, we failed to observe any regulatory role for IRGM at regulating such a process (Figs 4A and EV5A). However, *GATE16* silencing increased their ability to respond to *Salmonella* through the non-canonical inflammasome (Figs 4A and EV5A). When we used Nigericin to trigger the canonical NLRP3 inflammasome, hMDMs knocked down for *GATE16* did not show cell death and IL-1B alterations (Fig 4B). To the contrary, *IRGM*-silenced hMDMs had

 

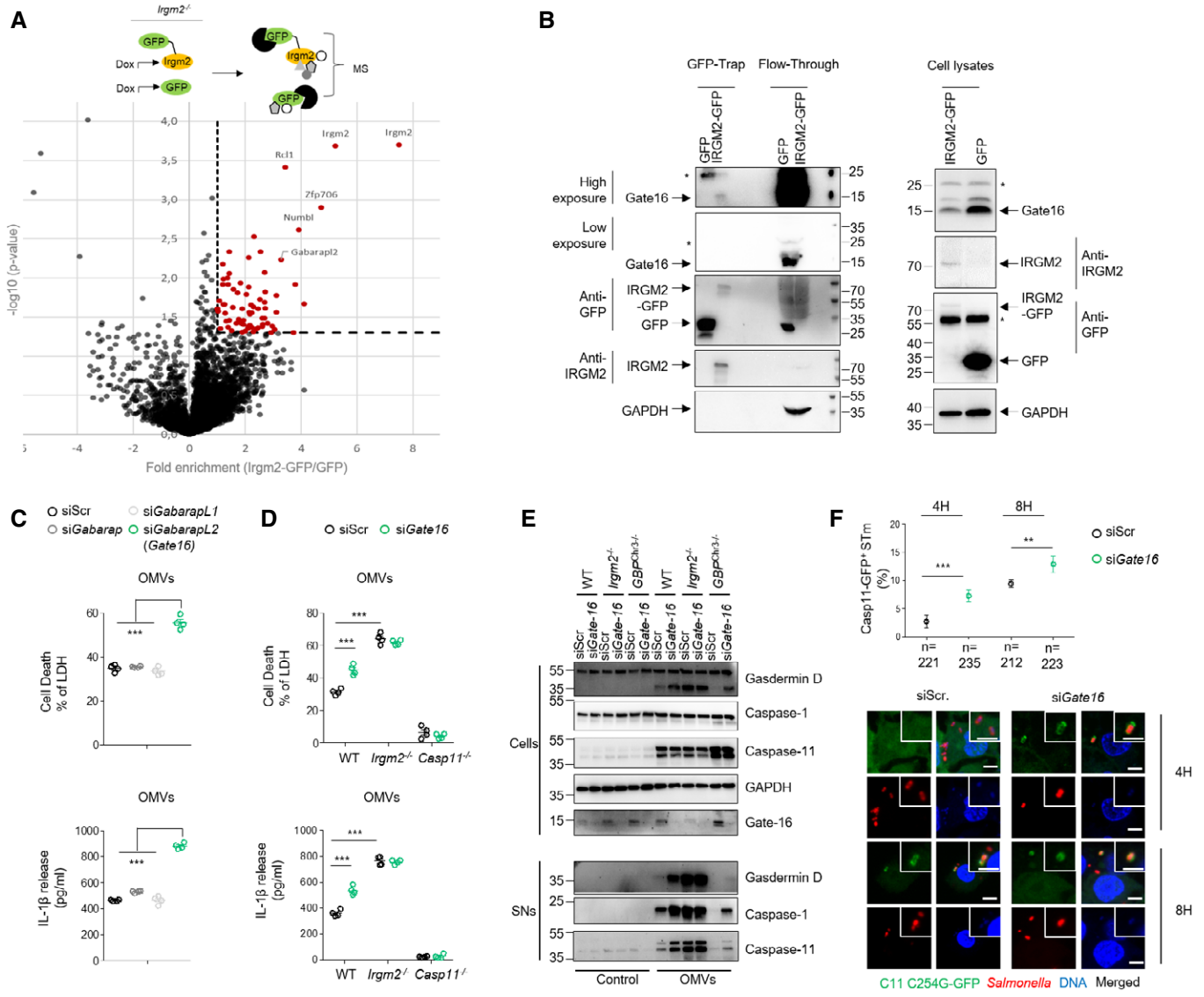


**Figure 3. Irgm2 cooperates with GATE16 to dampen Gram-negative bacteria-induced non-canonical inflammasome activation.**

A GFP-Trap coupled to mass spectrometry strategy used. The volcano plot represents three independent combined experiments. Threshold selection of enriched proteins (red dots) in Irgm2-GFP fraction was set at 2-fold enrichment (*x*-axis) and *P*-value < 0.05 (*y*-axis). Blacks and grey dots indicate proteins that did not reach a *P*-value < 0.05 using *t*-test with Bonferroni correction. Labelled proteins represent the top 6 enriched proteins in the Irgm2 fraction.

B Green florescent protein (GFP)-Trap assay of the presence of Gate16 in Irgm2-GFP-enriched fraction from the lysates of IFNγ-primed i*Irgm2*$^{-/-}$ BMDMs complemented with lentiviral constructs coding for a fusion of Irgm2 with GFP (Irgm2-GFP) or GFP alone. Arrows show the presence or not of Gate16, Irgm2-GFP and GAPDH in the Irgm2-GFP-enriched fractions, flow-through and total cell lysates. * means non-specific band.

C LDH and IL-1β release from siRNA-treated WT BMDMs, and then exposed to 2.5 μg/2 × $10^5$ cells of OMVs for 16 h.

D LDH and IL-1β release from WT, *Irgm2*$^{-/-}$ and *Casp11*$^{-/-}$ BMDMs silenced for *Gate16* and treated for 16 h with 2.5 μg/2 × $10^5$ cells of OMVs. Si Scramble (siScr.) refers to RNAi pools with non-targeting sequences.

E Western blot examination of caspase-11 and processed caspase-1 (p20) and gasdermin-D (p30) in supernatants and pro-caspase-1 (p45), pro-gasdermin-D (p55), pro-caspase-11, Gate16 and GAPDH in cell lysates of *Gate16*-silenced WT, *Irgm2*$^{-/-}$ and *GBP*$^{Chr3-/-}$ BMDMs exposed to 2.5 μg/2 × $10^5$ cells of OMVs for 16 h. Si Scramble (siScr.) refers to RNAi pools with non-targeting sequences.

F Representative confocal fluorescence microscopy images and associated quantifications of caspase-11-C254G-GFP (green) recruitment to *S.* Tm-mCherry (*orgA*$^{-}$, red, MOI 10) in IFNγ-primed iWT BMDMs silenced for *Gate16* after 4 and 8 h of infection. Nucleus (blue) was stained with Hoechst, scale bar 5 μm. For quantifications, the percentage of bacteria positive for caspase-11-C254G-GFP was determined by combining the bacterial counts from *n* = 3 independent experiments and expressed as mean ± SEM. ***P* ≤ 0.01, ****P* ≤ 0.001 for the indicated comparisons using *t*-test with Bonferroni correction. Si Scramble (siScr.) refers to RNAi pools with non-targeting sequences.

Data information: Data shown as means ± SEM (graphs C, D) from *n* = 4 independent pooled experiments; ****P* ≤ 0.001 for the indicated comparisons using *t*-test with Bonferroni correction. Image (B) is representative of one experiment performed two times, and (E) represents one experiment out of three. (A) represents one experiment out of three independent experiments.
Source data are available online for this figure.

higher IL-1B and cell death levels than their respective controls, which is reminiscent of previous studies that showed a regulatory role for IRGM on the canonical NLRP3 inflammasome (Fig 4B). Although the research of a protein with a similar function of rodent Irgm2 in humans warrants further investigations, our results suggest that GATE16 function is conserved between both species. Next, we wondered if GATE16-inhibited non-canonical inflammasome response to *Salmonella* depended on human GBPs. GBP1, GBP2 and GBP5 have recently been described as being important for efficient CASP4 recruitment and activation on bacterial membranes. Hence, we used human monocytic cell line U937 genetically invalidated for GBP1, GBP2 and GBP5 (*GBP1/2/5*$^{-/-}$) (Fig EV5B). Infection of IFNγ-primed WT or *GBP1/2/5*$^{-/-}$ U937 cells with *Salmonella* triggered both GBP-dependent cell death and IL-1B release (Fig 4C). Importantly, *GATE16* silencing in *GBP1/2/5*$^{-/-}$ cells reinsured significant cell death and IL-1B release, suggesting that the human non-canonical inflammasome response relies on GBP-dependent and GBP-independent mechanisms (Fig 4C). Finally, we aimed at determining if GATE16 is a direct regulator of the non-canonical inflammasome response in human cells. Therefore, we electroporated LPS in WT or *GBP1/2/5*$^{-/-}$ U937 cells in the presence or absence of *GATE16* siRNA (Fig 4D). Our results showed that electroporated LPS-induced cell death and IL1B release did not involve GATE16 (Fig 4D), suggesting that GATE16 acts upstream of the non-canonical inflammasome. Altogether, our results identified Irgm2 and GATE16 that cooperatively restrict Gram-negative bacteria-induced non-canonical inflammasome activation in both mice and humans.

Tight regulation of the non-canonical inflammasome pathway is of major importance as its uncontrolled non-canonical inflammasome response drives endotoxic shock. Conversely, two recent studies have uncovered that the IRF2 transcription factor (and to a lower extent IRF1) transcriptionally controls murine gasdermin-D and human caspase-4 expression (Benaoudia *et al*, 2019; Kayagaki *et al*, 2019). In addition, SERPINB1 has also been found to directly interact and inhibit activation of the inflammatory caspase-1, caspase-4 and caspase-11 (Choi *et al*, 2019). Here, both Finethy *et al* (2020) and us report a critical role of Irgm2 and Gate-16 at balancing the non-canonical inflammasome activity. The Irgm2/Gate-16 axis was required to inhibit caspase-11 recruitment to Gram-negative bacteria in the host cell cytosol, which provided controlled caspase-11 response and protection against sepsis. These findings open many yet unanswered questions such as at which step the Irgm2/Gate16 axis is regulating caspase-11 recruitment to bacterial products. Gate-16 has been found to control proper cytosolic localization of various GBPs (Park *et al*, 2016; Sasai *et al*, 2017), including GBP2, crucial at regulating caspase-11 recruitment on intracellular pathogen PAMPs. However, results from Finethy *et al* (2020) and ours indicate that *Gate16/Irgm2* removal in GBP-deficient macrophages (lacking GBPs 1, 2, 3, 5 and 7) partially restores a caspase-11-dependent response, suggesting that the Gate-16/Irgm2 path might regulate caspase-11, at least to certain extent, independently of these GBPs. Recently, two publications described that hGBP4 participated with GBP1 and GBP3 to the recruitment of CASP4 to cytosolic Gram-negative bacterial membranes in human

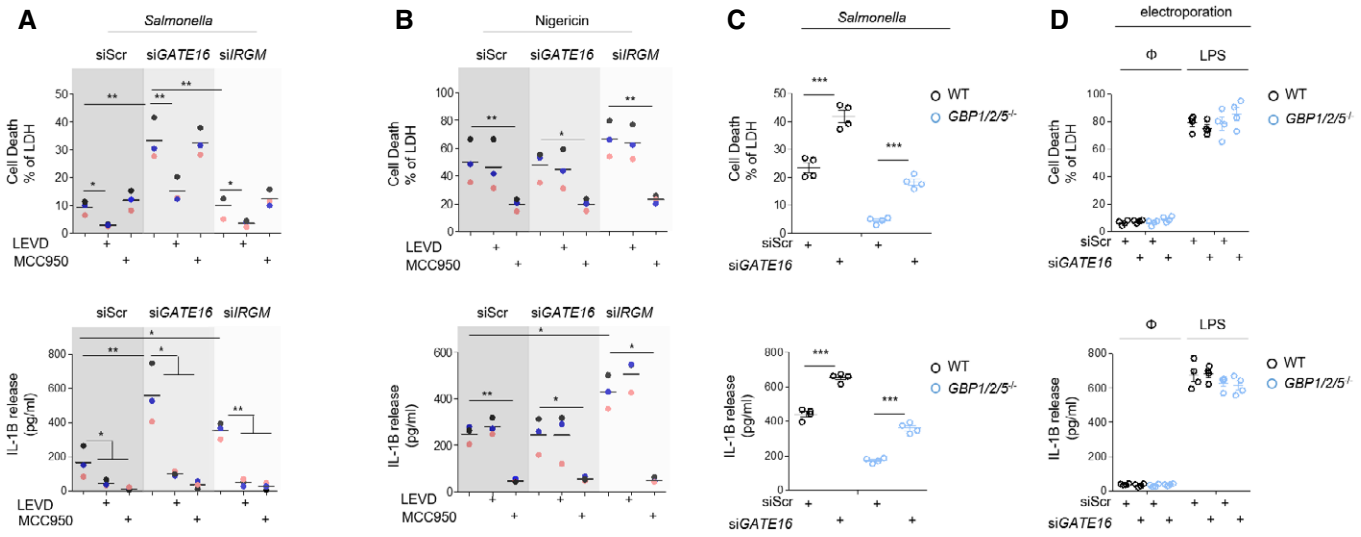


**Figure 4. GATE16 inhibits non-canonical inflammasome activation in human myeloid cells.**

A LDH and IL-1B release from siRNA-treated primary human monocyte-derived macrophages (hMDMs) infected with *S.* Typhimurium *orgA*$^{-}$ (MOI25) for 16 h. When specified, the caspase-4/5 inhibitor Z-LEVD (25 μM) or the NLRP3 inhibitor MCC950 (10 μM) was added to the experiments.

B LDH and IL-1B release from siRNA-treated primary human monocyte-derived macrophages (hMDMs), primed with IFNγ (10 UI/ml) and PAM3CSK4 (100 ng/ml) and then stimulated with Nigericin (20 μM) for 4 h. When specified, the caspase-4/5 inhibitor Z-LEVD (25 μM) or the NLRP3 inhibitor MCC950 (10 μM) was added to the experiments.

C, D LDH and IL-1B release from siRNA-treated WT or *GBP1/2/5*$^{-/-}$ U937 monocytic cell line, primed with IFNγ (10 UI/ml) and PAM3CSK4 (100 ng/ml) and then infected with (C) with *S.* Typhimurium *orgA*$^{-}$ (MOI25) for 10 h or (D) electroporated with 1 μg of *Escherichia coli* LPS for 4 h. Φ indicates that no LPS electroporation was performed. Data shown as means ± SEM from $n = 4$ independent pooled experiments; ***$P \leq 0.001$ for the indicated comparisons using *t*-test with Bonferroni correction.

Data information: Data shown as means (graphs A, B) from $n = 3$ different donors; each donor is represented with a coloured circle; *$P \leq 0.05$, **$P \leq 0.01$ for the indicated comparisons using one-way ANOVA with multiple Bonferroni correction.

epithelial cells (Santos *et al*, 2020; Wandel *et al*, 2020). Whether Irgm2/Gate-16-inhibited caspase-11 (or hCASP4) enrichment on bacterial membranes involves other GBPs (4 and 6) remains to be addressed. So far, due to the lack of information, a possible function of Irgm2 remains elusive, but Irgm1 and its human homologous IRGM have been described to participate in the autophagy/xenophagy processes (Maric-Biresev *et al*, 2016; Azzam *et al*, 2017). In addition, Gate-16 belongs to the ATG8-like proteins, including LC3 (abc), Gabarap and GabarapL1, all involved in various autophagy/membrane remodelling step regulation such as lysosome biogenesis, autophagosome formation and closure (Lee & Lee, 2016; Nguyen *et al*, 2016; Gu *et al*, 2019). To this regard, both Irgm1/IRGM (Finethy *et al*, 2020) and Gabarap proteins inhibit the activation of the Nlrp3 inflammasome (Pei *et al*, 2017; Mehto *et al*, 2019a,b). In addition, Irgm-1 and Irgm-3 deficiencies also rescue exacerbated inflammasome response from Irgm2-deficient macrophages (Finethy *et al*, 2020). Therefore, one can hypothesize that *Gate-16* and *Irgm2* deficiencies could lead to defective autophagy, which would promote cytosolic LPS accumulation and an exacerbated caspase-11 activation. However, results from Finethy *et al* (2020) and our own suggest that Gate-16 and Irgm2 regulate Gram-negative bacteria-induced non-canonical inflammasome response in an autophagy-independent manner. Should those effectors modulate the non-canonical autophagy pathway is an attractive hypothesis that deserves further investigations. Another possible explanation relies on the Golgi enrichment of both Irgm2 and Gate-16 (Sagiv, 2000; Zhao *et al*, 2010). Indeed, Gate-16 also regulates Snare-dependent vesicular trafficking, independently of its autophagy function (Sagiv, 2000). Various groups previously found that endocytosed and intracellular monomeric LPS could be targeted to the Golgi apparatus (Thieblemont & Wright, 1999; Latz *et al*, 2002). Caspase-4, caspase-5 and caspase-11 need accessible lipid A to oligomerize and auto activate, which can be extremely difficult in the presence of multimeric and hydrophobic LPS particles to the contrary of monomeric LPS that might present a more accessible lipid A. An attractive hypothesis is that GBP-mediated bacterial membrane damages allow LPS retrieval from aggregates in order to ensure proper lipid A exposure to caspase-11 (Santos *et al*, 2018, 2020; Kutsch *et al*, 2020; Wandel *et al*, 2020). Therefore, one could speculate that Golgi-regulated monomeric LPS trafficking might be impaired in the absence of either Irgm2 or Gate-16, which would allow direct caspase-11/lipid A interactions without the need for GBPs.

Our results showed that both murine and human Gate-16 regulate the non-canonical inflammasome response to LPS-containing particles. Yet, we failed to isolate IRGM as a human functional homologous of Irgm2. Given the strong role of Irgm2 at regulating the non-canonical inflammasome in mice, there is a possibility that another, yet unidentified, human protein holds a similar function of the one carried out by Irgm2. Therefore, this warrants future investigations to identify such Irgm2-like human protein. Humans and mice have different sensitivities to LPS. Indeed, LPS-induced sepsis in mice requires 1–25 mg/kg of LPS whereas humans have a 100–1,000,000 time lower sepsis threshold (2–4 ng/kg of LPS) (Fink, 2014). Another explanation could be that the evolutionary loss of Irgm2 in humans would leave human cells with only Gate-16, which would greatly lower the sensitivity of human cells to cytosolic LPS-activated non-canonical inflammasome.

In summary, our work identified two negative regulators of caspase-11 recruitment to bacterial membranes, namely Irgm2 and Gate-16. Additional investigations will be necessary to understand how both effectors balance caspase-4, caspase-5 and caspase-11 sensitivity to Gram-negative bacteria, and what specific physiological and cellular processes Irgm2 and Gate-16 cover together.

## Materials and Methods

Reagents, biological samples and their concentration of use are referenced in the Appendix Table S1.

### Mice

*Casp11*$^{-/-}$, *Casp1*$^{-/-}$*Casp11*$^{-/-}$, *Nlrp3*$^{-/-}$ and *GBP*$^{\mathrm{Chr3}-/-}$ mice have been described in previous studies (Li *et al*, 1995; Wang *et al*, 1998; Martinon *et al*, 2006; Yamamoto *et al*, 2012). *Irgm2*$^{-/-}$ mice were provided by the Jackson laboratory (USA). All mice were bred at the IPBS institute (Toulouse, France) animal facilities according to the EU and French directives on animal welfare (Directive 2010/63/EU). Charles Rivers provided WT C57BL/6J and C57BL/6N mice.

### Animal sepsis models

8- to 12-week-old mice (sex-matched, 6–10 per group) were injected intraperitoneally with a solution of 100 µl of poly(IC) LMW (invivoGen, 100 µg/animal) for 6 h. Then, mice were intraperitoneally injected with 5 mg/kg of LPS (InvivoGen, O111:B4) or 5 or 25 µg/animal of outer membrane vesicles (*E. coli*, InvivoGen). Mouse survival was monitored over 80 h. For cytokine assays, poly(IC)-primed mice were injected with 25 µg/animal of OMVs for 8 h and plasma cytokine amounts were addressed using ELISA kits (listed in the Appendix Table S1). There was no randomization or blinding performed.

Animal experiments were approved (Licence APAFIS#8521-2017041008135771, Minister of Research, France) and performed according to local guidelines (French ethical laws) and the European Union animal protection directive (Directive 2010/63/EU).

### BMDM isolation and culture

Murine bone marrow-derived macrophage (BMDM) generation has previously been described. Briefly, bone marrow progenitors were differentiated in DMEM (Invitrogen) supplemented with 10% *v/v* FCS (Thermo Fisher Scientific), 10% *v/v* MCSF (L929 cell supernatant), 10 mM HEPES (Invitrogen) and nonessential amino acids (Invitrogen) for 7 days. For experiments, $1.25 \times 10^6$, $2.5 \times 10^5$ or $5 \times 10^4$ BMDMs were seeded in 6-, 24- or 96-well plates, respectively, when described BMDMs were prestimulated overnight with either PAM3CSK4 (InvivoGen, 100 ng/ml) or IFNγ (PeProtech, 100 UI/ml). For non-canonical inflammasome stimulation, we used pure LPS (O111B4, InvivoGen, 1 µg/ml), outer membrane vesicles (*E. coli*, InvivoGen, 0.5, 1 and 2.5 µg/$2 \times 10^5$ cells) or various Gram-negative bacterial strains were used including, *Shigella flexneri* (M90T, MOI25), *Salmonella* Typhimurium *orgA*$^-$ (SL1344, MOI25), *E. coli* (K12, MOI25), *Citrobacter koseri* (MOI25) and *Enterobacter cloacae* (MOI25). When required, Wortmannin (Wort, 10 µM) and 3-metyladenine (3-MA, 1 mM) were added 2 h after infection in order to inhibit autophagy. When

specified, 1 μg of *E. coli* ultrapure LPS (O111:B4) was electroporated with Neon™ Transfection System (Thermo Fisher) according to manufacturer's protocol. Briefly, $5 \times 10^5$ cells were resuspended in Buffer R and 1 μg/ml of LPS was electroporated in 10 μl tips using two pulses of 1,720 V and 10 width. Cells were then plated in 24-well plates.

For canonical inflammasome stimulations, overnight (ON) IFNγ-primed BMDMs were then prestimulated with PAM3CSK4 (InvivoGen, 100 ng/ml) for 4 h to induce pro-IL1β expression. Then, Nigericin (NLRP3 activator, 40 μM, InvivoGen), dA:dT (AIM2 activator, 1 μg/ml, InvivoGen), TcdB toxin (PYRIN inducer, 0.05 μg/ml, List Biological Laboratories) or flagellin (NLRC4 trigger, 1 μg/ml, InvivoGen) was used to stimulate various canonical inflammasomes. Both flagellin and poly(dA:dT) were transfected into cells using FuGeneHD (Promega) transfection reagent in Opti-MEM culture medium. When specified, *P. aeruginosa* (PAO1) and *S*. Tm strains (SL1344) (MOI 5) were used to trigger NLRC4 inflammasome response.

For all stimulations, macrophage medium was replaced by serum-free and antibiotic-free Opti-MEM medium and inflammasome triggers were added to the macrophages for various times.

Specific to infections, plates were centrifuged for 1 min, 800 rpm to ensure homogenous infections. Then, extracellular bacteria were eliminated with gentamicin (100 μg/ml, Invitrogen).

#### Bacterial cultures

Bacteria were grown overnight in Luria Broth (LB) medium at 37°C with aeration and constant agitation in the presence or absence of antibiotics (specified in the Appendix Table S1), stationary phase (OD of 2–2.5) bacteria when then used for infections. Stimulation of the NLRC4 inflammasome by *S*. Typhimurium SL1344 and *P. aeruginosa* PAO1 bacteria required proper T3SS and flagellin expression; therefore, bacteria were sub-cultured the next day by dilution overnight culture 1/50 and grew until reaching an O.D600 of 0.6–1.

#### CFU evaluation

$2.5 \times 10^5$ BMDMs were infected with stationary phase *Salmonella orgA*$^-$ (MOI10) for 1 h. Cells were treated with gentamicin (100 μg/ml) for 30 min to kill extracellular bacteria and then washed three times in PBS. Medium was replaced with BMDM medium supplemented with 20 μg/ml of gentamicin to avoid extracellular bacterial replication. At the end of the experiment, cells were lysed in Triton 0.1% and intracellular bacterial loads were evaluated using CFU plating.

#### Gene knock down

Gene silencing was achieved using siRNA pools (Dharmacon, 25 nM/well listed in Appendix Table S1) as previously described (Meunier *et al*, 2015; Santos *et al*, 2018) or accell siRNA technology. SiRNA smart pools from Dharmacon were transfected into cells using the DharmaFECT 4 transfection reagent (Dharmacon) for 48 h. Primary human macrophages were treated with 1 μM siRNA Accell (Dharmacon, smart pool) in the absence of transfection reagent for 72 h. Then, murine BMDMs and human macrophages were stimulated with 1 μg/$2 \times 10^5$ cells of OMVs or infected with *Salmonella* Typhimurium (*orgA*$^-$) to trigger non-canonical inflammasome response. For siRNA experiments, gene knock down efficiency was monitored by qRT–PCR or immunoblotting (WB) assays.

#### Quantitative real-time PCR

Cellular RNAs were extracted from $2.5 \times 10^5$ cells using RNeasy Mini Kit (Qiagen). mRNAs were reverse transcribed with the Verso cDNA Synthesis Kit (Thermo Scientific). Regarding qPCR experiments, 1 μM of primers (Appendix Table S1), SYBR™ Select Master Mix (Thermo Scientific) and 15 ng of cDNA were mixed in a 10 μl reaction in a QuantStudio 5 device (Applied Biosystems). Primers were generated using primer3 software.

#### Cytokine and pyroptosis measurement

Murine Il-1α, IL-1β, TNF-α, IL12, IL18, IFNγ, IL-6, and human IL-1B cytokine levels were measured by ELISA (listed in Appendix Table S1). LDH cytotoxicity detection kit (Takara) allowed to monitor for cell lysis. Normalization of spontaneous lysis was calculated as follows: (LDH infected − LDH uninfected)/(LDH total lysis − LDH uninfected) × 100.

#### Immunoblotting

Preparation of cell lysates and supernatants has been described previously. Proteins were loaded and separated in 12% SDS–PAGE gels and then transferred on PVDF membranes. After 1 h of saturation in Tris-buffered saline (TBS) with 0.05% Tween 20 containing 5% non-fat milk (pH 8), membranes were incubated overnight with various antibodies (referenced in Appendix Table S1). The next day, membranes were washed three times in TBS 0.1% Tween 20 and incubated with appropriate secondary horseradish peroxidase (HRP)-conjugated antibody (dilution 1/5,000–10,000, listed in Appendix Table S1) for 1 h at room temperature. Then, after three washes, immunoblottings were revealed with a chemiluminescent substrate ECL substrate (Bio-Rad) and images were acquired using ChemiDoc Imaging System (Bio-Rad). All antibody references and working dilutions are presented in Appendix Table S1.

#### Microscopy

$2.5 \times 10^5$ BMDMs on glass coverslips were infected with *S*. Typhimurium (MOI10) expressing an mCherry fluorescent protein. At the indicated times, cells were washed three times with PBS and fixed with 4% PFA for 10 min at 37°C. 0.1 M glycine was used to quench excess of PFA for 10 min at room temperature. Then, cells were permeabilized and incubated with primary antibodies O/N at 4°C in saponin 0.1%/BSA 3% solution. Cellular stainings were achieved using Hoescht (DNA labelling), GBP2 antibody (gift from J Howard). Coverslips were then washed with Saponin/BSA solution and further incubated with the appropriate secondary antibodies coupled to fluorochromes (1/1,000; Appendix Table S1). After three washes with PBS, cells were mounted on glass slides using VECTASHIELD (Vectalabs). Coverslips were imaged using confocal Zeiss LSM 710 (Image core Facility, IPBS, Toulouse or an Olympus/Andor CSU-X1 Spinning dick microscope using a 63× oil objective. Otherwise specified, 5–10 fields/experiment were manually counted using ImageJ software.

 

### Transduction of iBMDMs

HEK 293-based retroviral packaging cell line (GP2-293) was plated in 10-cm Petri dish in DMEM + 10% FCS + 1% PS. When cell's confluency reached 60–80%, cells were placed in serum and antibiotic-free Opti-mem medium and transfected with VSV-G encoding vector (pMD.2G) along with CASP11-C254G-GFP or pRetro (-GFP or –Irgm2-GFP) vectors using PEI transfection reagent. 10 h after transfection, cell medium was replaced by DMEM + 10% FCS + 1% PS. At 48 h post-transfection, cell's supernatant containing retroviral particles were collected, filtered 0.45 μm and used to transduce target cells. After 48 h, puromycin (5 μg/ml) was used to select cells positively transduced with the transgene. When vectors contained GFP fusions, cells were sorted using fluorescence-activated cell sorting.

### Immunoprecipitation and GFP-Trap

*Irgm2*$^{-/-}$ immortalized macrophages were transduced with retroviral vectors carrying a doxycycline-inducible Irgm2-GFP, or GFP alone constructs, cloned into Retro-X™ Tet-On® 3G vector (Clontech Laboratories, Inc.). To ensure proper Irgm2-GFP expression, cells were incubated 16 h with doxycycline 1 μg/ml in the presence of IFNγ. Irgm2-GFP and associated protein complexes were pull-down using GFP-Trap magnetic beads according to manufacturer's instructions (chromotek). Briefly, cells were lysed in CoIP lysis buffer (10 mM Tris/Cl pH 7.5; 150 mM NaCl; 0.5 mM EDTA; 0.5% NP-40, 0.09% Na-Azide) supplemented with a protease inhibitor cocktail (Roche). Cell lysates were then incubated with GFP-Trap-MA beads for 1 h at 4°C. After two washes with wash-buffer (10 mM Tris/Cl pH 7.5; 150 mM NaCl; 0.5 mM EDTA, 0.018% Na-Azide), GFP-Trap complexes were boiled for 10 min at 95°C in RIPA buffer + Laemmli before separation on SDS–PAGE and mass spectrometry or immunoblotting.

### Mass spectrometry analysis

Immuno-purified protein samples were reduced with β-mercaptoethanol by heating at 95°C for 5 min, and cysteines were alkylated by addition of 90 mM iodoacetamide. Samples were loaded on a 1D SDS–PAGE gel, and proteins were isolated in a single gel band, which was excised and washed with several cycles of 50 mM ammonium bicarbonate–acetonitrile (1:1). Proteins were in-gel digested using 0.6 μg of modified sequencing grade trypsin (Promega) in 50 mM ammonium bicarbonate overnight at 37°C. Resulting peptides were extracted from the gel by successive incubations in 50 mM ammonium bicarbonate and 10% formic acid–acetonitrile (1:1), then dried in a speed-vac and resuspended with 22 μl of 5% acetonitrile, 0.05% trifluoroacetic acid (TFA) for MS analysis. Peptides were analysed by nanoLC-MS/MS using an UltiMate Nano/Cap System NCS-3500RS coupled to a Q-Exactive HFX mass spectrometer (Thermo Fisher Scientific, Bremen, Germany). Separation was performed on a C-18 column (75 μm ID × 50 cm, Reprosil C18) equilibrated in 95% solvent A (5% acetonitrile, 0.2% formic acid) and 5% solvent B (80% acetonitrile, 0.2% formic acid), using a gradient from 10 to 45% gradient of solvent B over 60 min at a flow rate of 350 nl/min. The mass spectrometer was operated in data-dependent acquisition mode with the Xcalibur software. Survey MS scans were acquired in the Orbitrap on the 350–1,400 $m/z$ range, with the resolution set to 60,000, and the 12 most intense ions were selected for fragmentation by higher-energy collisional dissociation (HCD) using a normalized collision energy of 28. MS/MS scans were collected at 15,000 resolution with an AGC target value of 1e5 and a maximum injection time of 22 ms. Dynamic exclusion was used within 30 s to prevent repetitive selection of the same peptide. Three replicate MS analyses were performed for each sample.

### Bioinformatic processing of mass spectrometry data

Raw mass spectrometry files were searched using Mascot (Matrix Science) against the Mouse entries of the SwissProt–TrEmbl protein database. The enzyme specificity was "trypsin", with a maximum of two misscleavages. Cysteine carbamidomethylation was set as a fixed modification, and N-terminal protein acetylation and methionine oxidation were specified as variable modifications. For the search, mass tolerance parameters were set at 5 ppm on the parent ion and 20 mmu on the fragment ions. Protein identification results were then validated with the Proline software by the target-decoy approach using a reverse database at a both a peptide and a protein FDR of 1%. To perform label-free relative quantification of proteins, the "abundance" metric retrieved by Proline was used, after global normalization of the MS signal across all MS runs. For each protein, a mean abundance value was computed from technical LC-MS replicate runs, and $\log_2$-transformed. Missing protein abundance values were then replaced by a noise value estimated for each analysis as the 1% lowest percentile of the protein abundance values distribution. Bona fide Irgm2 interactors were identified by comparing Irmg2-GFP immuno-purified samples and GFP control samples. For each protein, an enrichment ratio relative to the control and a Student *t*-test *P*-value was calculated from the protein abundance values derived from three independent biological replicate experiments. Relevant interactors were selected based on an enrichment ratio higher than 2 and a Student *t*-test *P*-value lower than 0.05.

### Genetic invalidation of *Caspase-11* and *Irgm2* genes in immortalized BMDMs

*Casp11* and *Irgm2* genes were knocked out using the crispr/cas9 system in onco J2-immortalized (i) bone marrow-derived macrophages (BMDMs) iWTs or i*Irgm2*$^{-/-}$macrophages. Single guide RNAs (sgRNA) specifically targeting caspase-11 exon 2 forward (5′CACCGCTTAAGGTGTTGGAACAGCT3′) reverse (5′AAACAGCTG TTCCAACACCTTAAGC3′), Irgm2 exon 2 forward (5′CACCGTTCCA TGTTGTCGAGCAACG3′) reverse (5′AAACCGTTGCTCGACAACATG GAAC3′) were designed using Benchling tool (Benchling.com), and oligonucleotides were synthesized by Sigma-Aldrich. Crispr guide RNA oligonucleotides were then hybridized and cloned in LentigRNA-Puromycin vector using BsmBI restriction enzyme (lentiGuide-Puro, Addgene 52963, Feng Zhang Lab). HEK293T cells were transfected for 48 h with all constructs (Lipofectamine 2000) together with the lentiviral packaging vector p8.91 (Didier Trono Lab, EPFL, Switzerland) and the envelop coding VSV-G plasmid (pMD.2G, Addgene 12259, Didier Trono Lab). 48 h later, viral supernatants were harvested and subsequently filtered on 0.45-μm filter. Recipient cells expressing Cas9 (1,000,000 cells/well in 6-well plates) were generated using lentiviral transduction with a Cas9-expressing lentiviral vector (lentiCas9-Blast, Addgene 52962, Feng Zhang Lab). Then, Cas9$^+$ cells were infected with packaged viral

particles. To ensure efficient infection, viral particles were centrifugated for 2 h at 1,081 *g* at 32°C in presence of 8 μg/ml polybrene. 48 h later, medium was replaced and puromycin selection (10 μg/ml) was applied to select positive clones for 2 weeks. Puromycin-resistant cells were sorted at the single-cell level by FACS (Aria cell sorter). Individual clones were subjected to Western blotting to confirm the absence of targeted proteins.

#### Genetic invalidation of human GBPs in U937 cell line

To generate GBP1/2/5 knock-out cell line, deletion of genes was performed in a Cas9-expressing U937 clone obtained by transduction with the plasmid LentiCas9-Blast (from Feng Zhang; Addgene plasmid # 52962) followed by blasticidin selection and clonal isolation using the limit dilution method. A clone strongly expressing Cas9 was selected based on Western blot analysis using anti-Cas9 antibody (Millipore; # MAC133; 1:1,000 dilution). gRNAs targeting GBP1, GBP2 and GBP5 (Appendix Table S1) were cloned into the pKLV-U6gRNA(BbsI)-PGKpuro2ABFP vector (from Kosuke Yusa; Addgene plasmid # 50946). For each gene, two pairs of gRNAs were used. Lentiviral particles were produced in 293T cells using pMD2.G and psPAX2 (from Didier Trono, Addgene plasmids #12259 and #12260), and pKLV-U6gRNA(BbsI)-PGKpuro2ABFP. Cas9-expressing U937 cells were transduced by spinoculation. Gene deletion invalidation was verified by Western blotting analysis (Appendix Table S1).

#### Generation of human monocyte-derived macrophages

Peripheral blood mononuclear cells (PBMCs) were isolated from buffy coat of healthy donors obtained from the EFS Toulouse Purpan (France). Briefly, PBMCs were isolated by centrifugation using standard Ficoll-Paque density (GE Healthcare). The blood was diluted 1:1 in phosphate-buffered saline (PBS) pre-warmed to 37°C and carefully layered over the Ficoll-Paque gradient. The tubes were centrifuged for 25 min at 514 *g*, at 20°C. The cell interface layer was harvested carefully, and the cells were washed twice in PBS (for 10 min at 185 *g* followed by 10 min at 800 rpm) and resuspended in RPMI-1640 supplemented with 10% of foetal calf serum (FCS), 1% penicillin (100 IU/ml) and streptomycin (100 μg/ml). Monocytes were separated from lymphocytes by positive selection using $CD14^+$ isolation kit (Miltenyi Biotec). To allow differentiation into monocyte-derived macrophages, cells were cultured in RPMI medium (GIBCO) supplemented with 10% FCS (Invitrogen), 100 IU/ml penicillin, 100 μg/ml streptomycin and 10 ng/ml MCSF for 7 days.

#### Ethics statements

The use of human cells was approved by the Research Ethical Committee, Haute-Garonne, France. Buffy coats were provided anonymously by the EFS (établissement français du sang, Toulouse, France). Written informed consent was obtained from each donor under EFS contract no 21PLER2017-0035AV02, according, to "Decret No 2007-1220 (articles L1243-4, R1243-61)".

#### Statistical analysis

Statistical data analysis was performed using Prism 5.0a (GraphPad Software, Inc.). *t*-Test with Bonferroni correction was used for comparison of two groups. For multiple comparisons, one-way ANOVA with multiple Bonferroni correction test was used. Data are reported as mean with SEM. For animal experiments, Mann–Whitney tests were performed, and for mouse survival analysis, log-rank Cox–Mantel test was selected. *P*-values are given in figures, NS means non-significant. Significance is specified as $*P \leq 0.05$; $**P \leq 0.01$, $***P \leq 0.001$.

## Data availability

The mass spectrometry proteomic data have been deposited to the ProteomeXchange Consortium via the PRIDE (Perez-Riverol *et al*, 2019) partner repository with the data set identifier PXD020457 (http://proteomecentral.proteomexchange.org/cgi/GetDataset?ID=PXD020457).

**Expanded View** for this article is available online.

### Acknowledgements
We would like to acknowledge Biotem company for generating anti-Irgm2 antibodies; Junying Yuan (Harvard Med School, Boston, USA) and B. Py (CIRI institute, Lyon, France) for sharing *Caspase1*$^{-/-}$*Caspase11*$^{-/-}$ and *Caspase11*$^{-/-}$ mice (Li *et al*, 1995; Wang *et al*, 1998); V. Petrilli and B. Py for providing the *Nlrp3*$^{-/-}$ mice (Martinon *et al*, 2006). *Irgm2*$^{-/-}$ mice came from the Jackson laboratory. The authors also acknowledge the animal facility, mass spectrometry and microscopy platforms of the IPBS institute. We specifically acknowledge Drs. A. Gonzalez de Peredo for mass spectrometry data processing, G. Lugo-Villarino, C. Cougoule and Y. Rombouts for fruitful discussions and suggestions as well as for reading and implementing the MS. This project was funded by grants from FRM "Amorçage Jeunes Equipes" (AJE20151034460), ERC StG (INFLAME 804249) and ATIP to EM and from the European Society of Clinical Microbiology and Infectious Diseases (ESCMID) to RP. MY (Masahiro Yamamoto) is supported by the Research ProGram on Emerging and Re-emerging Infectious Diseases (JP19fk0108047), Japanese Initiative for Progress of Research on Infectious Diseases for global Epidemic (JP19fm0208018) and Strategic International Collaborative Research ProGram (19jm0210067h) from Agency for Medical Research and Development (AMED), Grant-in-Aid for Scientific Research on Innovative Areas (Production, function and structure of neo-self; 19H04809), for Scientific Research (B) (18KK0226 and 18H02642) and for Scientific Research (A) (19H00970) from Ministry of Education, Culture, Sports, Science and Technology of Japan.

### Author contributions
EE and EM designed the experiments with the help of RP. EE, RP and EM wrote the manuscript. EE and RP performed the experiments with the help of SB, P-JB, AH, KS and MP. KC and OB-S performed essential mass spectrometry run acquisitions and analysis. TH, BL, MY and JCH provided essential reagents to conduct the project.

### Conflict of interest
The authors declare that they have no conflict of interest.

## References

Aachoui Y, Leaf IA, Hagar JA, Fontana MF, Campos CG, Zak DE, Tan MH, Cotter PA, Vance RE, Aderem A *et al* (2013) Caspase-11 protects against bacteria that escape the vacuole. *Science* 339: 975 – 978

 

Aglietti RA, Estevez A, Gupta A, Ramirez MG, Liu PS, Kayagaki N, Ciferri C, Dixit VM, Dueber EC (2016) GsdmD p30 elicited by caspase-11 during pyroptosis forms pores in membranes. *Proc Natl Acad Sci USA* 113: 7858 – 7863

Azzam KM, Madenspacher JH, Cain DW, Lai L, Gowdy KM, Rai P, Janardhan K, Clayton N, Cunningham W, Jensen H *et al* (2017) Irgm1 coordinately regulates autoimmunity and host defense at select mucosal surfaces. *JCI Insight* 2: e91914

Basters A, Knobeloch KP, Fritz G (2018) USP18 – a multifunctional component in the interferon response. *Biosci Rep* 38: BSR20180250

Benaoudia S, Martin A, Puig Gamez M, Gay G, Lagrange B, Cornut M, Krasnykov K, Claude J, Bourgeois CF, Hughes S *et al* (2019) A genome-wide screen identifies IRF2 as a key regulator of caspase-4 in human cells. *EMBO Rep* 20: e48235

Broz P, Ruby T, Belhocine K, Bouley DM, Kayagaki N, Dixit VM, Monack DM (2012) Caspase-11 increases susceptibility to *Salmonella* infection in the absence of caspase-1. *Nature* 490: 288 – 291

Cerqueira DM, Gomes MTR, Silva ALN, Rungue M, Assis NRG, Guimarães ES, Morais SB, Broz P, Zamboni DS, Oliveira SC (2018) Guanylate-binding protein 5 licenses caspase-11 for Gasdermin-D mediated host resistance to Brucella abortus infection. *PLoS Pathog* 14: e1007519

Chen KW, Monteleone M, Boucher D, Sollberger G, Ramnath D, Condon ND, von Pein JB, Broz P, Sweet MJ, Schroder K (2018) Noncanonical inflammasome signaling elicits gasdermin D–dependent neutrophil extracellular traps. *Sci Immunol* 3: eaar6676

Cheng KT, Xiong S, Ye Z, Hong Z, Di A, Tsang KM, Gao X, An S, Mittal M, Vogel SM *et al* (2017) Caspase-11-mediated endothelial pyroptosis underlies endotoxemia-induced lung injury. *J Clin Invest* 127: 4124 – 4135

Choi YJ, Kim S, Choi Y, Nielsen TB, Yan J, Lu A, Ruan J, Lee HR, Wu H, Spellberg B *et al* (2019) SERPINB1-mediated checkpoint of inflammatory caspase activation. *Nat Immunol* 20: 276 – 287

Coers J (2013) Self and non-self discrimination of intracellular membranes by the innate immune system. *PLoS Pathog* 9: e1003538

Costa Franco MM, Marim F, Guimarães ES, Assis NRG, Cerqueira DM, Alves-Silva J, Harms J, Splitter G, Smith J, Kanneganti T-D *et al* (2018) Brucella abortus triggers a cGAS-independent STING pathway to induce host protection that involves guanylate-binding proteins and inflammasome activation. *J Immunol* 200: 607 – 622

Deng M, Tang Y, Li W, Wang X, Zhang R, Zhang X, Zhao X, Liu J, Tang C, Liu Z *et al* (2018) The endotoxin delivery protein HMGB1 mediates caspase-11-dependent lethality in sepsis. *Immunity* 49: 740 – 753

Feeley EM, Pilla-Moffett DM, Zwack EE, Piro AS, Finethy R, Kolb JP, Martinez J, Brodsky IE, Coers J (2017) Galectin-3 directs antimicrobial guanylate binding proteins to vacuoles furnished with bacterial secretion systems. *Proc Natl Acad Sci USA* 114: E1698 – E1706

Finethy R, Jorgensen I, Haldar AK, De Zoete MR, Strowig T, Flavell RA, Yamamoto M, Nagarajan UM, Miao EA, Coers J (2015) Guanylate binding proteins enable rapid activation of canonical and noncanonical inflammasomes in Chlamydia-infected macrophages. *Infect Immun* 83: 4740 – 4749

Finethy R, Luoma S, Orench-Rivera N, Feeley EM, Haldar AK, Yamamoto M, Kanneganti T-D, Kuehn MJ, Coers J (2017) Inflammasome activation by bacterial outer membrane vesicles requires guanylate binding proteins. *MBio* 8: e01188-17

Finethy R, Dockterman J, Kutsch M, Orench-Rivera N, Wallace G, Piro A, Luoma S, Haldar AK, Hwang S, Martinez J *et al* (2020) Dynamin-related Irgm proteins modulate LPS-induced caspase-11 activation and septic shock. *EMBO Rep* 21: e50830

Fink MP (2014) Animal models of sepsis. *Virulence* 5: 143 – 153

Fisch D, Bando H, Clough B, Hornung V, Yamamoto M, Shenoy AR, Frickel E (2019) Human GBP 1 is a microbe-specific gatekeeper of macrophage apoptosis and pyroptosis. *EMBO J* 38: e100926

Green R, Ireton RC, Gale M (2018) Interferon-stimulated genes: new platforms and computational approaches. *Mamm Genome* 29: 593 – 602

Gu Y, Princely Abudu Y, Kumar S, Bissa B, Choi SW, Jia J, Lazarou M, Eskelinen E, Johansen T, Deretic V (2019) Mammalian Atg8 proteins regulate lysosome and autolysosome biogenesis through SNAREs. *EMBO J* 38: e101994

Hagar JA, Powell DA, Aachoui Y, Ernst RK, Miao EA (2013) Cytoplasmic LPS activates caspase-11: implications in TLR4-independent endotoxic shock. *Science* 341: 1250 – 1253

Haldar AK, Saka HA, Piro AS, Da Dunn J, Henry SC, Taylor GA, Frickel EM, Valdivia RH, Coers J (2013) IRG and GBP host resistance factors target aberrant, "non-self" vacuoles characterized by the missing of "Self" IRGM proteins. *PLoS Pathog* 9: e1003414

Haldar AK, Foltz C, Finethy R, Piro AS, Feeley EM, Pilla-Moffett DM, Komatsu M, Frickel EM, Coers J (2015) Ubiquitin systems mark pathogen-containing vacuoles as targets for host defense by guanylate binding proteins. *Proc Natl Acad Sci USA* 112: E5628 – E5637

Hayward JA, Mathur A, Ngo C, Man SM (2018) Cytosolic recognition of microbes and pathogens: inflammasomes in action. *Microbiol Mol Biol Rev* 82: e00015-18

Kayagaki N, Warming S, Lamkanfi M, Walle LV, Louie S, Dong J, Newton K, Qu Y, Liu J, Heldens S *et al* (2011) Non-canonical inflammasome activation targets caspase-11. *Nature* 479: 117 – 121

Kayagaki N, Wong MT, Stowe IB, Ramani SR, Gonzalez LC, Akashi-takamura S, Miyake K, Zhang J, Lee WP, Forsberg LS *et al* (2013) Independent of TLR4. *Science* 130: 1246 – 1249

Kayagaki N, Stowe IB, Lee BL, O'Rourke K, Anderson K, Warming S, Cuellar T, Haley B, Roose-Girma M, Phung QT *et al* (2015) Caspase-11 cleaves gasdermin D for non-canonical inflammasome signalling. *Nature* 526: 666 – 671

Kayagaki N, Lee BL, Stowe IB, Kornfeld OS, O'Rourke K, Mirrashidi KM, Haley B, Watanabe C, Roose-Girma M, Modrusan Z *et al* (2019) IRF2 transcriptionally induces GSDMD expression for pyroptosis. *Sci Signal* 12: eaax4917

Kim BH, Shenoy AR, Kumar P, Bradfield CJ, MacMicking JD (2012) IFN-inducible GTPases in host cell defense. *Cell Host Microbe* 12: 432 – 444

Kim S, Eun H, Jo E-K (2019) Roles of autophagy-related genes in the pathogenesis of inflammatory bowel disease. *Cells* 8: 77

Kutsch M, Sistemich L, Lesser CF, Goldberg MB, Herrmann C, Coers J (2020) Direct binding of polymeric GBP1 to LPS disrupts bacterial cell envelope functions. *EMBO J* 39: e104926

Lagrange B, Benaoudia S, Wallet P, Magnotti F, Provost A, Michal F, Martin A, Di Lorenzo F, Py BF, Molinaro A *et al* (2018) Human caspase-4 detects tetra-acylated LPS and cytosolic Francisella and functions differently from murine caspase-11. *Nat Commun* 9: 242

Latz E, Visintin A, Lien E, Fitzgerald KA, Monks BG, Kurt-Jones EA, Golenbock DT, Espevik T (2002) Lipopolysaccharide rapidly traffics to and from the golgi apparatus with the toll-like receptor 4-MD-2-CD14 complex in a process that is distinct from the initiation of signal transduction. *J Biol Chem* 277: 47834 – 47843

Lee YK, Lee JA (2016) Role of the mammalian ATG8/LC3 family in autophagy: differential and compensatory roles in the spatiotemporal regulation of autophagy. *BMB Rep* 49: 424 – 430

Lee BL, Stowe IB, Gupta A, Kornfeld OS, Roose-Girma M, Anderson K, Warming S, Zhang J, Lee WP, Kayagaki N (2018) Caspase-11 auto-

 

proteolysis is crucial for noncanonical inflammasome activation. *J Exp Med* 215: 2279 – 2288

Li P, Allen H, Banerjee S, Franklin S, Herzog L, Johnston C, McDowell J, Paskind M, Rodman L, Salfeld J *et al* (1995) Mice deficient in IL-1β-converting enzyme are defective in production of mature IL-1β and resistant to endotoxic shock. *Cell* 80: 401 – 411

Liau NPD, Laktyushin A, Lucet IS, Murphy JM, Yao S, Whitlock E, Callaghan K, Nicola NA, Kershaw NJ, Babon JJ (2018) The molecular basis of JAK/STAT inhibition by SOCS1. *Nat Commun* 9: 1 – 14

Liu X, Zhang Z, Ruan J, Pan Y, Magupalli VG, Wu H, Lieberman J (2016) Inflammasome-activated gasdermin D causes pyroptosis by forming membrane pores. *Nature* 535: 153 – 158

Liu BC, Sarhan J, Panda A, Muendlein HI, Ilyukha V, Coers J, Yamamoto M, Isberg RR, Poltorak A (2018) Constitutive interferon maintains GBP expression required for release of bacterial components upstream of pyroptosis and anti-DNA responses. *Cell Rep* 24: 155 – 168

Man SM, Karki R, Malireddi RKS, Neale G, Vogel P, Yamamoto M, Lamkanfi M, Kanneganti TD (2015) The transcription factor IRF1 and guanylate-binding proteins target activation of the AIM2 inflammasome by Francisella infection. *Nat Immunol* 16: 467 – 475

Man SM, Karki R, Sasai M, Place DE, Kesavardhana S, Temirov J, Frase S, Zhu Q, Malireddi RKS, Kuriakose T *et al* (2016) IRGB10 liberates bacterial ligands for sensing by the AIM2 and Caspase-11-NLRP3 inflammasomes. *Cell* 167: 382 – 396

Maric-Biresev J, Hunn JP, Krut O, Helms JB, Martens S, Howard JC (2016) Loss of the interferon-γ-inducible regulatory immunity-related GTPase (IRG), Irgm1, causes activation of effector IRG proteins on lysosomes, damaging lysosomal function and predicting the dramatic susceptibility of Irgm1-deficient mice to infection. *BMC Biol* 14: 33

Martinon F, Pétrilli V, Mayor A, Tardivel A, Tschopp J (2006) Gout-associated uric acid crystals activate the NALP3 inflammasome. *Nature* 440: 237 – 241

Masud S, Prajsnar TK, Torraca V, Lamers GEM, Benning M, Van Der Vaart M, Meijer AH (2019) Macrophages target Salmonella by Lc3-associated phagocytosis in a systemic infection model. *Autophagy* 15: 796 – 812

Mehto S, Chauhan S, Jena KK, Chauhan NR, Nath P, Sahu R, Dhar K, Das SK, Chauhan S (2019a) IRGM restrains NLRP3 inflammasome activation by mediating its SQSTM1/p62-dependent selective autophagy. *Autophagy* 15: 1645 – 1647

Mehto S, Jena KK, Nath P, Chauhan S, Kolapalli SP, Das SK, Sahoo PK, Jain A, Taylor GA, Chauhan S (2019b) The Crohn's disease risk factor IRGM limits NLRP3 inflammasome activation by impeding its assembly and by mediating its selective autophagy. *Mol Cell* 73: 429 – 445

Meunier E, Dick MS, Dreier RF, Schürmann N, Broz DK, Warming S, Roose-Girma M, Bumann D, Kayagaki N, Takeda K *et al* (2014) Caspase-11 activation requires lysis of pathogen-containing vacuoles by IFN-induced GTPases. *Nature* 509: 366 – 370

Meunier E, Wallet P, Dreier RF, Costanzo S, Anton L, Rühl S, Dussurgey S, Dick MS, Kistner A, Rigard M *et al* (2015) Guanylate-binding proteins promote activation of the AIM2 inflammasome during infection with Francisella novicida. *Nat Immunol* 16: 476 – 484

Napier BA, Brubaker SW, Sweeney TE, Monette P, Rothmeier GH, Gertsvolf NA, Puschnik A, Carette JE, Khatri P, Monack DM (2016) Complement pathway amplifies caspase-11-dependent cell death and endotoxin-induced sepsis severity. *J Exp Med* 213: 2365 – 2382

Nguyen TN, Padman BS, Usher J, Oorschot V, Ramm G, Lazarou M (2016) Atg8 family LC3/GAB ARAP proteins are crucial for autophagosome-lysosome fusion but not autophagosome formation during PINK1/Parkin mitophagy and starvation. *J Cell Biol* 215: 857 – 874

Park S, Choi J, Biering SB, Dominici E, Williams LE, Hwang S (2016) Targeting by AutophaGy proteins (TAG): targeting of IFNG-inducible GTPases to membranes by the LC3 conjugation system of autophagy. *Autophagy* 12: 1153 – 1167

Pei C, Wang C, Xu H (2017) Irgm1 suppresses NLRP3 Inflammasome-mediated IL-1β production. *J Immunol* 198 (1 Supplement): 201.25

Pilla DM, Hagar JA, Haldar AK, Mason AK, Degrandi D, Pfeffer K, Ernst RK, Yamamoto M, Miao EA, Coers J (2014) Guanylate binding proteins promote caspase-11-dependent pyroptosis in response to cytoplasmic LPS. *Proc Natl Acad Sci USA* 111: 6046 – 6051

Pilla-Moffett D, Barber MF, Taylor GA, Coers J (2016) Interferon-inducible GTPases in host resistance, inflammation and disease. *J Mol Biol* 428: 3495 – 3513

Rathinam VAK, Zhao Y, Shao F (2019) Innate immunity to intracellular LPS. *Nat Immunol* 20: 527 – 533

Rühl S, Broz P (2015) Caspase-11 activates a canonical NLRP3 inflammasome by promoting K+ efflux. *Eur J Immunol* 45: 2927 – 2936

Rühl S, Shkarina K, Demarco B, Heilig R, Santos JC, Broz P (2018) ESCRT-dependent membrane repair negatively regulates pyroptosis downstream of GSDMD activation. *Science* 362: 956 – 960

Sagiv Y (2000) GATE-16, a membrane transport modulator, interacts with NSF and the Golgi v-SNARE GOS-28. *EMBO J* 19: 1494 – 1504

Santos JC, Dick MS, Lagrange B, Degrandi D, Pfeffer K, Yamamoto M, Meunier E, Pelczar P, Henry T, Broz P (2018) LPS targets host guanylate-binding proteins to the bacterial outer membrane for non-canonical inflammasome activation. *EMBO J* 37: e98089

Santos JC, Boucher D, Schneider LK, Demarco B, Dilucca M, Shkarina K, Heilig R, Chen KW, Lim RYH, Broz P (2020) Human GBP1 binds LPS to initiate assembly of a caspase-4 activating platform on cytosolic bacteria. *Nat Commun* 11: 1 – 15

Sasai M, Sakaguchi N, Ma JS, Nakamura S, Kawabata T, Bando H, Lee Y, Saitoh T, Akira S, Iwasaki A *et al* (2017) Essential role for GABARAP autophagy proteins in interferon-inducible GTPase-mediated host defense. *Nat Immunol* 18: 899 – 910

Sborgi L, Rühl S, Mulvihill E, Pipercevic J, Heilig R, Stahlberg H, Farady CJ, Müller DJ, Broz P, Hiller S (2016) GSDMD membrane pore formation constitutes the mechanism of pyroptotic cell death. *EMBO J* 35: 1766 – 1778

Schmid-Burgk JL, Gaidt MM, Schmidt T, Ebert TS, Bartok E, Hornung V (2015) Caspase-4 mediates non-canonical activation of the NLRP3 inflammasome in human myeloid cells. *Eur J Immunol* 45: 2911 – 2917

Shi J, Zhao Y, Wang K, Shi X, Wang Y, Huang H, Zhuang Y, Cai T, Wang F, Shao F (2015) Cleavage of GSDMD by inflammatory caspases determines pyroptotic cell death. *Nature* 526: 660 – 665

Perez-Riverol Y, Csordas A, Bai J, Bernal-Llinares M, Hewapathirana S, Kundu DJ, Inuganti A, Griss J, Mayer G, Eisenacher M *et al* (2019) The PRIDE database and related tools and resources in 2019: improving support for quantification data. *Nucleic Acids Res* 2019 47: D442 – D450

Thieblemont N, Wright SD (1999) Transport of bacterial lipopolysaccharide to the Golgi apparatus. *J Exp Med* 190: 523 – 534

Thurston TLM, Matthews SA, Jennings E, Alix E, Shao F, Shenoy AR, Birrell MA, Holden DW (2016) Growth inhibition of cytosolic Salmonella by caspase-1 and caspase-11 precedes host cell death. *Nat Commun* 7: 1 – 15

Vanaja SK, Russo AJ, Behl B, Banerjee I, Yankova M, Deshmukh SD, Rathinam VAK (2016) Bacterial outer membrane vesicles mediate cytosolic localization of LPS and Caspase-11 activation. *Cell* 165: 1106 – 1119

Wallet P, Benaoudia S, Mosnier A, Lagrange B, Martin A, Lindgren H, Golovliov I, Michal F, Basso P, Djebali S *et al* (2017) IFN-γ extends the immune functions of Guanylate Binding Proteins to inflammasome-

 

independent antibacterial activities during Francisella novicida infection. *PLoS Pathog* 13: e1006630

Wandel MP, Kim BH, Park ES, Boyle KB, Nayak K, Lagrange B, Herod A, Henry T, Zilbauer M, Rohde J *et al* (2020) Guanylate-binding proteins convert cytosolic bacteria into caspase-4 signaling platforms. *Nat Immunol* 21: 880 – 891

Wang S, Miura M, Jung YK, Zhu H, Li E, Yuan J (1998) Murine caspase-11, an ICE-interacting protease, is essential for the activation of ICE. *Cell* 92: 501 – 509

Wu Y-W, Li F (2019) Bacterial interaction with host autophagy. *Virulence* 10: 352 – 362

Yamamoto M, Okuyama M, Ma JS, Kimura T, Kamiyama N, Saiga H, Ohshima J, Sasai M, Kayama H, Okamoto T *et al* (2012) A cluster of interferon-γ-inducible p65 gtpases plays a critical role in host defense against toxoplasma gondii. *Immunity* 37: 302 – 313

Yang J, Zhao Y, Shao F (2015) Non-canonical activation of inflammatory caspases by cytosolic LPS in innate immunity. *Curr Opin Immunol* 32: 78 – 83

Yang X, Cheng X, Tang Y, Qiu X, Wang Y, Kang H, Wu J, Wang Z, Liu Y, Chen F *et al* (2019) Bacterial endotoxin activates the coagulation cascade through gasdermin D-dependent phosphatidylserine exposure. *Immunity* 51: 983 – 996

Zhao YO, Könen-Waisman S, Taylor GA, Martens S, Howard JC (2010) Localisation and mislocalisation of the interferon-inducible immunity-related GTPase, Irgm1 (LRG-47) in mouse cells. *PLoS ONE* 5: e8648

Zwack EE, Feeley EM, Burton AR, Hu B, Yamamoto M, Kanneganti TD, Bliska JB, Coers J, Brodsky IE (2017) Guanylate binding proteins regulate inflammasome activation in response to hyperinjected Yersinia translocon components. *Infect Immun* 85: e00778-16